Journal of the Korean Chemical Society
2011, *Vol. 55, No. 3*
Printed in the Republic of Korea
DOI 10.5012/jkcs.2011.55.3.364

0.25 M 황산 용액 상에서의 Imatinib Mesylate에 의한 연강철 부식 억제

K. N. Mohana*, S. S. Shivakumar, and A. M. Badiea
Department of Studies in Chemistry, University of Mysore, Manasagangotri, Mysore 570 006, India
(접수 2011. 1. 3; 수정 2011. 1. 13; 게재확정 2011. 3. 10)

Inhibition of Mild Steel Corrosion in 0.25 M Sulphuric Acid Solution by Imatinib Mesylate

K. N. Mohana*, S. S. Shivakumar, and A. M. Badiea
Department of Studies in Chemistry, University of Mysore, Manasagangotri, Mysore 570 006, India.
**E-mail: knmsvp@yahoo.com*
(Received January 3, 2011; Revised January 13, 2011; Accepted March 10, 2011)

요 약. 다양한 억제제의 농도, 온도, 유속에서 중량 분석과 변전위 분극법을 이용하여 0.25 M 황산 용액상에 있는 연강철에 대한 imatinib mesylate (IMT)의 부식 억제를 연구하였다. 억제제의 농도가 증가함에 따라 억제 효과가 증가한다는 결과를 얻었다. 연강철 표면 위의 흡착 과정은 Langmuir 흡착 등온선을 따른다. 얻어진 흡착 깁스 자유 에너지의 값은 연강철 위의 IMT의 흡착 과정이 화학흡착이라는 것을 보여준다. 열역학 변수들이 계산되고, 논의되었다. IMT의 HOMO와 LUMO의 전자궤도 밀도 분포는 억제 메커니즘을 논의하는데 이용되었다. FT-IR 분광학과 SEM 이미지는 필름에 흡착된 표면을 분석하기 위해 사용되었다.

주제어: 연강철, Imatinib mesylate, 황산 매질, 분극, 흡착

ABSTRACT. The corrosion inhibition of imatinib mesylate (IMT) on mild steel in 0.25 M sulphuric acid has been studied using gravimetric and potentiodynamic polarization techniques at various concentrations of inhibitor, temperature and fluid velocities. The results obtained showed that, inhibition efficiency (% IE) increases with increasing concentration of the inhibitor. The adsorption process on mild steel surface follows Langmuir adsorption isotherm. The values of Gibbs free energies of adsorption obtained suggest that, the adsorption process of IMT on mild steel is chemisorption. Thermodynamic parameters were evaluated and discussed. The electron orbital density distribution of HOMO and LUMO of IMT was used to discuss the inhibition mechanism. FT-IR spectroscopy and SEM images were used to analyze the surface adsorbed film.
Keywords: Mild steel, Imatinib mesylate, Sulphuric acid medium, Polarization, Adsorption

INTRODUCTION

The investigation of corrosion of mild steel is always a subject of high theoretical as well as practical interest. Mild steel is widely used in industries due to its good mechanical property. Sulphuric acid is most frequently used for the removal of undesirable scale and rust in metal finishing industries, heat exchangers, cleaning of boilers and pickling of iron and steel.[1-4] Corrosion inhibitors are often used to inhibit corrosion of apparatus caused by acid medium in many industrial operations.[5] Most of the well known acid inhibitors are organic compounds such as those containing nitrogen, sulphur, oxygen atoms and aromatic rings.[6-12] These substances in general are effective through adsorption on the metal surface. Compounds containing both nitrogen and sulphur groups generally give rise to satisfactory inhibition efficiency in the case of iron corrosion in acid medium.[13-15] The efficiency of these inhibitors depends on chemical composition and structure of the inhibitors and on the state of the metallic surface.[16,17] A few investigations have been reported on the use of drugs as corrosion inhibitors. Rhodanine azosulpha drugs have been reported to be corrosion inhibitors for the corrosion of 304 stainless steel in HCl medium.[18] They showed good corrosion inhibition by parallel adsorption on the surface of steel due to the presence of more than one active centre in the inhibitor. Some antibacterial drugs viz., ampicillin (AMP), cloxacillin, flucloxacillin and amoxicillin have been studied as inhibitors for the corrosion.[19] The corrosion inhibition of the mild steel in HCl medium by four sulpha drugs viz., sulfaguanidine, sulfamethazine, sulfamethoxazole and sulfadiazine was reported using both

weight loss and galvanostatic polarization.[20]

Accordingly, the aim of present work is to study the inhibitive performance of imatinib mesylate (IMT Cancer drug) on the corrosion of mild steel in 0.25 M sulphuric acid using gravimetric measurements and potentiodynamic polarization studies. Thermodynamic parameters such as adsorption heat, adsorption entropy and adsorption free energy were obtained from the experimental data of the inhibition process at different temperatures, and pre-exponential factor at various inhibitor concentrations were calculated. The effect of activation energy on the corrosion rate of mild steel was discussed. The adsorbed film containing the investigated compound has been identified by FT-IR spectroscopy and SEM analysis. The inhibition mechanism has been discussed based on the electron orbital density distribution of HOMO and LUMO of IMT molecule.

EXPERIMENTAL

Materials

The experiments were performed with mild steel having the chemical composition (weight %), C 0.090, Mn 1.373, P 0.016, Si 0.322, Cr 0.062, S 0.025 and the reminder iron. Imatinib mesylate (IMT) was procured from Intermed Labs, Bangalore, India. The chemical structure of IMT is shown in *Fig*. 1. A stock solution of IMT (10 mM) was prepared by weighing an appropriate amount of it and dissolved in 1 liter of 0.25 M H_2SO_4, and series of concentrations (1 mM - 5 mM) were prepared from this stock solution. Approximately 1 M H_2SO_4 solution was prepared by diluting the appropriate volume of the concentrated acid (AR grade) with double distilled water. The concentration of the acid was checked by titrating an appropriately diluted portion with standard solution of sodium hydroxide which was titrated in turn against standard solution of oxalic acid. From this stock concentrated solution, exactly 0.25 M H_2SO_4 solution was prepared by dilution with double distilled water which was used throughout the experiment.

Weight Loss Method

The reaction basin used in this method was a graduated glass vessel having a total capacity of 500 ml. 250 ml of the test solution was employed in each experiment. The test specimens were cut into 1×1×0.3 cm. They were mechanically polished with different grades of emery papers, degreased in acetone, rinsed with double distilled water and finally dried between two filter papers and weighed. Finally, they were kept in a desicator for 1 h until use. The temperature of the environment was maintained by thermostatically controlled water bath with accuracy of ± 0.2 C^0 (Weiber limited, Chennai, India). By using rotating disk method, the rotational speed of the specimen was set at desired speed by using speed regulator motor (Eltek Ltd, Mumbai, India). The one face of the specimen was exposed to solution and remaining faces were embedded with epoxy resin. After 6 h of immersion, three test pieces were taken out from the test solution, rinsed with double distilled water, dried as before and weighed again. The average weight loss for each set of three samples was taken. The weight loss was recorded to the nearest 0.0001 gram by using an analytical balance (Sartorius, precision ± 0.1 mg). The corrosion rates (CR) of mild steel were calculated at various rotational speeds (1800-2200 rpm) from mass loss using equation (1):

$$CR = \left(\frac{w}{A \times t}\right) \tag{1}$$

where W is the weight loss (mg), t is the immersion time (h), A is the surface area of the specimen in (cm^2) and CR is expressed in mg cm^{-2} h^{-1}.

The inhibition efficiency (% IE) and degree of surface coverage (θ) were calculated using the following equation:

$$\Theta = 1 - \frac{(CR)_p}{(CR)_a} \tag{2}$$

$$\%IE = \left(1 - \frac{(CR)_p}{(CR)_a} \times 100\right) \tag{3}$$

where $(CR)_p$ and $(CR)_a$ are the corrosion rate in the presence and absence of the inhibitor, respectively. The values of CR and % IE are given in *Table* 1.

Potentiodynamic Polarization Method

The electrochemical experiments were carried out in a three-electrode electrochemical cylindrical Pyrex glass cell with a platinum counter electrode and saturated calomel electrode (SCE) as reference. The working electrode had the form of a square cut from mild steel sheet. The square with an exposed area of 1 cm^2 which was then held in a shaft and rotated by motor driven shaft of ¼ hp. The

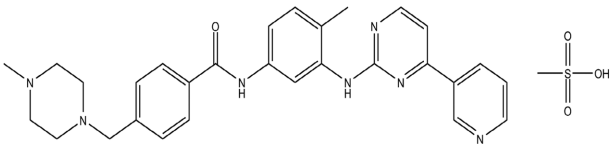

***Fig.* 1.** Chemical structure of IMT.

***Table* 1.** CR and %IE obtained from weight loss measurements of mild steel in sulphuric acid medium containing various concentrations of IMT at different temperatures and rotational speed

T, °C	C, mM	1800 rpm		2000 rpm		2200 rpm	
		CR, mg cm^{-2} h^{-1}	%IE	CR, mg cm^{-2} h^{-1}	%IE	CR, mg cm^{-2} h^{-1}	%IE
30	Blank	4.89	-	5.09	-	5.78	-
	1	2.66	45.54	2.81	44.69	3.19	44.75
	2	2.50	48.82	2.66	47.72	3.02	47.91
	4	1.69	65.27	1.80	64.62	2.10	63.77
	5	1.24	74.52	1.32	74.07	1.45	74.99
40	Blank	6.16	-	6.32	-	6.93	-
	1	2.99	51.41	3.14	50.37	3.51	49.40
	2	2.74	55.51	2.81	55.48	3.18	54.08
	4	1.80	70.79	1.90	69.88	2.15	68.94
	5	1.35	77.96	1.41	77.70	1.61	76.76
50	Blank	8.40	-	8.92	-	9.22	-
	1	3.35	60.11	3.71	58.44	4.35	52.78
	2	3.00	64.30	3.35	62.43	3.89	57.77
	4	2.06	75.51	2.26	74.68	2.70	70.73
	5	1.49	82.30	1.65	81.53	1.98	78.48
60	Blank	13.84	-	14.51	-	15.12	-
	1	4.97	64.09	5.38	63.74	5.89	61.09
	2	4.33	68.75	4.76	74.96	5.19	65.65
	4	2.31	83.33	2.51	83.62	2.77	81.67
	5	1.60	88.46	1.76	89.22	1.98	86.90
70	Blank	19.23	-	19.56	-	20.12	-
	1	6.84	64.46	7.09	58.46	7.99	60.25
	2	4.94	74.34	4.90	73.81	5.06	74.84
	4	2.91	84.90	3.20	81.75	3.66	81.82
	5	1.97	89.78	2.11	87.99	2.57	87.22
80	Blank	24.09	-	25.16	-	26.45	-
	1	9.64	60.00	10.36	58.82	11.22	57.58
	2	7.34	69.54	8.12	67.73	8.85	66.54
	4	5.60	76.73	6.05	75.95	6.72	74.60
	5	4.06	83.12	4.52	82.03	4.97	81.21

exposed area was polished with different grades of emery papers in the normal way starting from coarser to finer, followed by degreasing in acetone and finally washing with double distilled water, just before insertion in the electrolytic cell. A constant quantity of the test solution (100 ml) was taken in the polarization cell. A time interval of about 30 minutes was given for the system to attain a steady state and the open circuit potential (OCP) was noted. Both cathodic and anodic polarization curves were recorded potentiodynamically by changing the electrode potential between - 700 and + 500 mV from open circuit potential (OCP) at the scan rate of 0.4 mV s^{-1}, using potentiostat model Solatron 1286.

Inhibition efficiency was calculated from the electrochemical measurements by the following equation:

$$\%IE = \frac{(I_{cor})_a - (I_{cor})_p}{(I_{cor})_a} \times 100 \quad (4)$$

where $(I_{cor})_a$ and $(I_{cor})_p$ are the corrosion current density in the absence and presence of inhibitor, respectively. The corrosion potential (E_{cor}) and corrosion current density (I_{cor}) were calculated by extrapolation of anodic and cathodic Tafel slopes.

SEM analysis

Samples for SEM experiments are mild steel sheets (1 cm × 1 cm × 0.2 cm). After 6 h of immersion, the surface features of the steel specimens exposed to acid as well as inhibited acid were examined with the help of scanning electron microscope (model JSM-5800).

IR spectroscopy

The surface products deposited on the test specimens after 6 h of exposure at room temperature in the inhibited acid were analyzed by FTIR (JASCO FT-IR Spectrometer, model 4100) using KBr discs.

RESULTS AND DISCUSSION

Adsorption Isotherm

The dependence of the degree of surface coverage (θ) as function of concentration (C) of the inhibitor was tested graphically by fitting it to various isotherms to find the best isotherm which describes this study. Langmuir adsorption isotherm was found to be the best description for IMT on mild steel. According to this isotherm, θ is related to the inhibitor concentration, C and adsorption equilibrium constant K_{ads}, via[21]:

$$\frac{C}{\theta} = \frac{1}{K_{ads}} + C \tag{5}$$

The plot of C/θ versus C gave a straight line (*Fig.* 2) with a slope of around unity confirming that the adsorption of IMT on mild steel surface in sulphuric acid obeys the Langmuir adsorption isotherm. According to Langmuir adsorption isotherm there is no interaction between the adsorbed inhibitor molecules, and the energy of adsorption is independent on the degree of surface coverage (θ). Langmuir isotherm assumes that the solid surface contains a fixed number of adsorption sites and each site occupies one adsorbed species. The equilibrium adsorption constant, K_{ads} is related to the standard Gibb's free energy of adsorption (ΔG^0_{ads}) with the following equation:

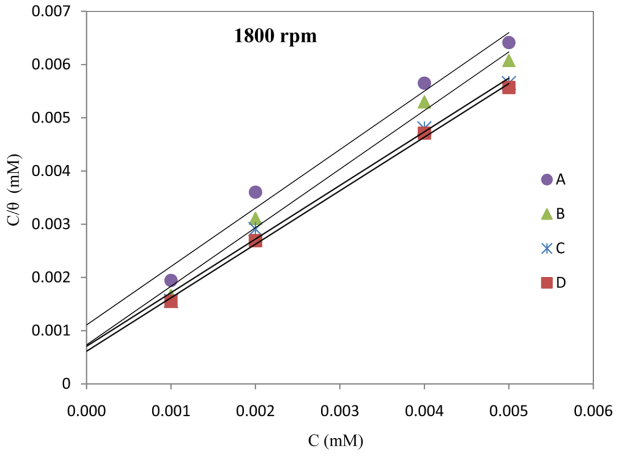

***Fig.* 2.** Langmuir's adsorption isotherm plots for the adsorption of IMT in 0.25 M H_2SO_4 on the surface of mild steel at A-313 K, B-323 K, C-333 K and D-343 K at 1800 rpm.

$$K_{ads} = \frac{1}{55.5}\exp\left[-\frac{\Delta G^0_{ads}}{RT}\right] \tag{6}$$

where 55.5 is the concentration of water in solution (mol L^{-1}), R is the universal gas constant and T is the absolute temperature. The enthalpy and entropy of adsorption (ΔH^0_{ads} and ΔS^0_{ads}) can be calculated using the equations (7) and (8).

$$\ln K_{ads} = \ln\left(\frac{1}{55.5}\right) - \frac{\Delta G^0_{ads}}{RT} \tag{7}$$

$$\ln K_{ads} = \ln\frac{1}{55.5} - \frac{\Delta H^0_{ads}}{RT} + \frac{\Delta S^0_{ads}}{R} \tag{8}$$

Using Eq. (8), the values of ΔH^0_{ads} and ΔS^0_{ads} were evaluated from the slope and intercept of the plot of ln K_{ads} versus 1/T (*Fig.* 3). The values of ΔG^0_{ads}, ΔH^0_{ads} and ΔS^0_{ads} are listed in *Table* 2. It shows that, the increase in K_{ads} with increasing temperature indicates increase in the extent of adsorption with temperature.[22] The negative values of ΔG^0_{ads} ensure the spontaneity of the adsorption process and stability of the adsorbed layer on the metal surface.[23] Generally, the values of ΔG^0_{ads} around - 20 kJ mol^{-1} or lower are consistent with the electrostatic interaction between the charged molecules and the charged metal (physisorption), while those around - 40 kJ mol^{-1} or higher indicate charge sharing or transfer from organic molecule to vacant 3d orbital of the metal to form co-ordinate type of bond (chemisorption).[24-25] In the present study, ΔG^0_{ads} values are more negative than -20 kJ mol^{-1} suggest that, the adsorption process of IMT on mild steel surface is typical chemisorption.[26] The value of ΔH^0_{ads} is another criterion to confirm the mode of adsorption. Generally, an exothermic adsorption process signifies either physisorp-

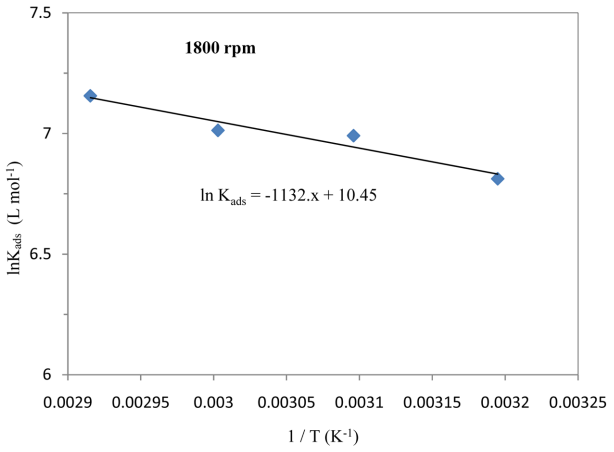

***Fig.* 3.** Plot of lnK_{ads} versus 1/T for IMT on mild steel in 0.25 M H_2SO_4 acid at 1800 rpm.

***Table* 2.** Thermodynamic parameters for adsorption of IMT on mild steel in 0.25 M sulphuric acid at different temperatures and 1800 rpm

T, K	R^2	K_{ads}, L mol^{-1}	ΔG^0_{ads}, kJ mol^{-1}	ΔH^0_{ads}, kJ mol^{-1}	ΔS^0_{ads}, J mol^{-1} K^{-1}
313	0.982	909.1	-28.18	9.41 [a]	120.27 [a]
323	0.990	1086.9	-29.56	9.39 [b]	120 [b]
343	0.993	1111.1	-30.54		
353	0.998	1282.1	-31.86		

[a]values obtained from Eq. (8) [b]values obtained from Eq. (9)

tion or chemisorption or mixture of both while an endothermic process is signifies chemisorption.[27] In the present case, the calculated value of ΔH^0_{ads} is 9.41 kJ mol^{-1} indicating chemisorption of IMT on metal surface. In fact, it is well known that adsorption is an exothermic phenomenon accompanied by a decrease in entropy.[28] In aqueous solution, the adsorption of organic molecule is generally accompanied with desorption of water molecules. The adsorption of an organic adsorbate at the metal/solution interface is considered a "substitutional adsorption" phenomenon.[29] Therefore, the positive values of ΔH^0_{ads} and ΔS^0_{ads} related to "substitutional adsorption".

The values of ΔH^0_{ads} and ΔS^0_{ads} can also be calculated by using following equation:

$$\Delta G^0_{ads} = \Delta H^0_{ads} - T\Delta S^0_{ads} \quad (9)$$

Using Eq. (9), the plot of ΔG^0_{ads} versus T gives a straight line with a slope of $-\Delta S^0_{ads}$ and intercept of ΔH^0_{ads}. The values obtained are well correlated with those obtained from Eq. (8).

Effect of Temperature

To assess the effect of temperature on corrosion and corrosion inhibition process, gravimetric experiments were performed at different temperatures (30-80 °C) in the absence and in the presence of various concentrations of the inhibitor during 6 h of immersion and at various rotational speeds (1800-2100 rpm) of the specimen. The results are presented in *Table* 1. From the *Fig.* 4 it is shown that, the CR increases with increasing the temperature in the absence of the inhibitor. However, this increase seems slightly in presence of the IMT. The relationship between the corrosion rate (CR) of mild steel and temperature (T) can be expressed by the Arrhenius equation:

$$CR = k \exp\left(-\frac{E_a^*}{RT}\right) \quad (10)$$

where E_a^* is the activation energy, k is the pre-exponential constant, R is the universal gas constant and T is the absolute temperature. Using Eq. (10), and from a plot of the log

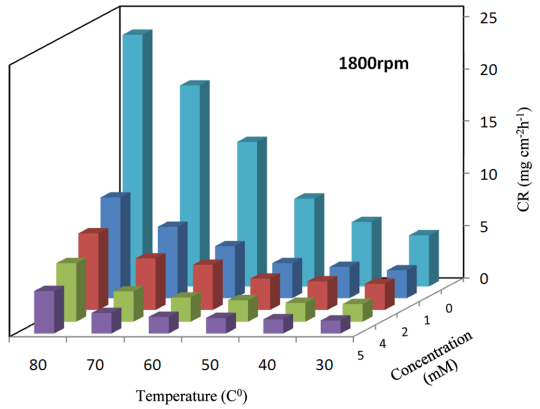

***Fig.* 4.** Variation of CR of mild steel as a function of temperature and concentration of IMT at 1800 rpm.

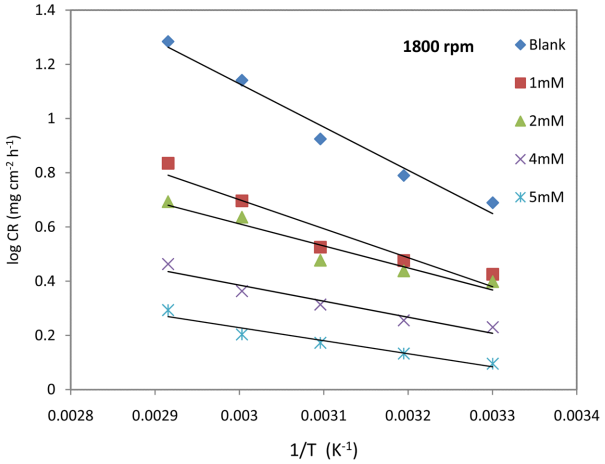

***Fig.* 5.** Plot of log CR versus 1/T for the corrosion of mild steel in 0.25 M H_2SO_4 containing various concentrations of IMT at 1800 rpm.

CR versus 1/T (*Fig.* 5), the values of E_a^* and k at various concentrations of IMT were computed from slopes and intercepts, respectively and the values are given in *Table* 3.

The lower value of E_a^* at higher inhibitor concentration was due to the slow rate of inhibitor adsorption.[30] Putilova[31] has reported that these types of inhibitors are effective at higher temperatures. Ampicillin (AMP), a beta-lactam antibiotic was studied as corrosion inhibitor for mild steel in 0.1 M H_2SO_4,[32] its inhibition efficiency decreases with increase in temperature. The inhibition efficiency of IMT

increases with temperature, because the addition of IMT to the acid solution decreases the activation energy. The reduction of the activation energy in the presence of IMT may be attributed to the chemisorption of the IMT on metal surface.[33-34] The increase of %IE with temperature is explained with the change in the adsorption character. In the present case physisorption has been observed at a lower temperature and transforms into chemisorption at higher temperature.[35] The adsorbed inhibitor molecules block significantly some of the active sites on the steel surface, which is energetically inhomogeneous. The inhibitor adsorbs at the active sites of the metal surface have the lowest E_a^* and other active sites of higher E_a^* will take part in the subsequent corrosion process.[36] The values of enthalpy and entropy of activation can be calculated from the alternative form of Arrhenius equation as follows:

$$CR = \frac{RT}{Nh}\exp\left(\frac{\Delta S_a^*}{R}\right)\exp\left(\frac{-\Delta H_a^*}{R}\right) \quad (11)$$

Where h is Planks constant, N is Avogadro's number, ΔS_a^* is the entropy of activation, ΔH_a^* is the enthalpy of activation. Plots of log (CR/T) versus 1/T gave straight lines (*Fig.* 6) with a slope of ($-\Delta H_a^* / 2.303R$) and an intercept of [log (R/Nh) + $\Delta S_a^*/2.303R$] from which the values of ΔH_a^* and ΔS_a^* were calculated and are listed in *Table* 3. The ΔH_a^* values obtained from the slope of Eq. (8) and those values calculated from the equation, $\Delta H_a^* = E_a^* - RT$ are in good agreement with each other. The positive values of ΔH_a^* both in the absence and presence of inhibitor reflect the endothermic nature of mild steel dissolution process.[37] The negative values of ΔS_a^* obtained indicate that the activated complex in the rate determining step represents an association rather than dissociation, means that decrease in the disorder of the system due to the adsorption of inhibitor molecule on to the metal surface.[38-40]

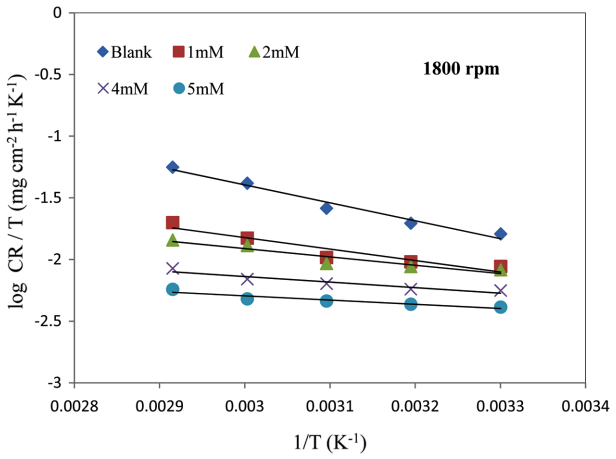

***Fig.* 6.** Alternative Arrhenius plots for mild steel dissolution in 0.25 M H_2SO_4 the absence and presence of different concentrations of IMT at 1800 rpm.

Effect of Rotational Speed

The corrosion measurements were carried out at different rotational speed of the specimen (1800-2000 rpm). From *Fig.* 7, it is clear that the %IE is maximum at 70 °C, 1800 rpm and at 5 mM IMT. Further, %IE increases with increasing rotational speed at all temperatures up to 1800 rpm however beyond 1800 rpm %IE decreases at all concentrations. Therefore, an optimum velocity is necessary for uniform distribution of an inhibitor.

Electrochemical Measurements

Potentiodynamic polarization curves obtained for the mild steel in 0.25 M sulphuric acid at various concentrations of IMT ranging from 1 mM to 5 mM are shown in

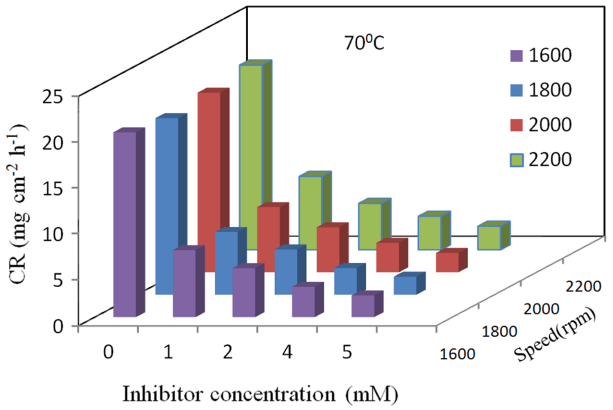

***Fig.* 7.** Variation of CR of mild steel as a function of rotational speed and concentration of IMT at 70 °C.

***Table* 3.** Values of activation parameters for mild steel in 0.25 M sulphuric acid medium in the absence and presence of IMT at 1800 rpm

C, mM	E_a, kJ mol^{-1}	k, mg cm^{-2} h^{-1}	ΔH_a, kJ mol^{-1}	$\Delta H_a = E_a$-RT, kJ mol^{-1}	ΔS_a, J mol^{-1} K^{-1}
blank	30.52	814704.28	27.84	28.00	-140.73
1mM	20.53	8090.95	17.79	17.92	-179.09
2mM	15.64	1122.01	12.88	12.95	-195.52
4mM	11.38	144.21	8.64	8.60	-212.91
5mM	9.25	46.88	6.52	6.40	-221.91

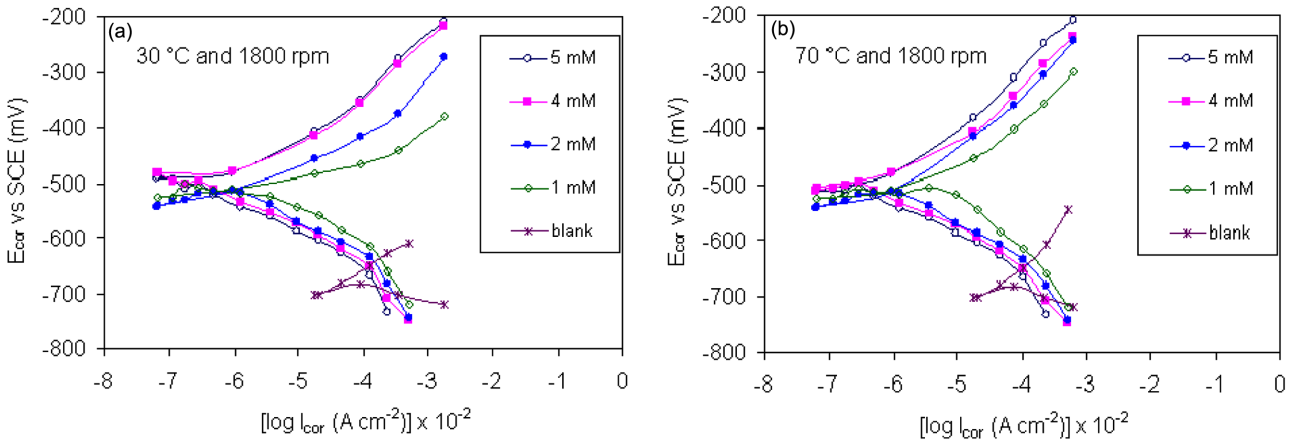

***Fig.* 8.** (a) Polarization curves for mild steel in 0.25 M H_2SO_4 containing different concentrations of IMT at 1800 rpm and 30 °C (scan rate = 0.42 mV s^{-1}), (b). Polarization curves for mild steel in 0.25M H_2SO_4 containing different concentrations of IMT at 1800 rpm and 70 °C (scan rate = 0.42 mV s^{-1}).

Figs. 8a and 8b. It can be observed that the addition of IMT at all the studied concentrations decreased the anodic and cathodic current densities, and resulted in significant decline in the I_{corr}. This indicates that IMT shifted to smaller I_{corr} values in both anodic and cathodic branches of the curves, thus, acting as a mixed-type inhibitor,[41] and the decrease is more pronounced with the increase in the inhibitor concentration at both temperatures. By comparing polarization curves in the absence and in the presence of various concentrations of IMT, it is observed that, increase in concentration of the inhibitor shift the corrosion potential (E_{corr}) in the positive direction and reduces both anodic and cathodic process.[38,42]

Molecule Structure and Inhibition Mechanism

The adsorption of IMT molecule in sulphuric acid may be due to the interaction between iron atom and cyclic molecular π orbital. The incompletely filled 3d orbital of iron could bond with highest occupied molecular orbital (HOMO)[43] of the IMT molecule, while the filled 4s orbital of the former could interact with the lowest unoccupied molecular orbital (LUMO) of the latter. This type of interaction has been explained in other documents.[44-45] The electron density distributions of HOMO and LUMO of IMT are shown in *Figs.* 9a and 9b. From this it can be seen that the larger HOMO (*Fig.* 9a) electron density at amide group and benzene ring are more feasible to interact with 3d orbital of iron, while the pyrimidine ring is having larger LUMO (*Fig.* 9b) electron density and could take priority of interaction with completely filled 4s orbital of iron. Both interactions lead to strong binding between iron and IMT and it evidence the negative value of ΔG^0_{ads}, and it increases with concentration. Another important factor

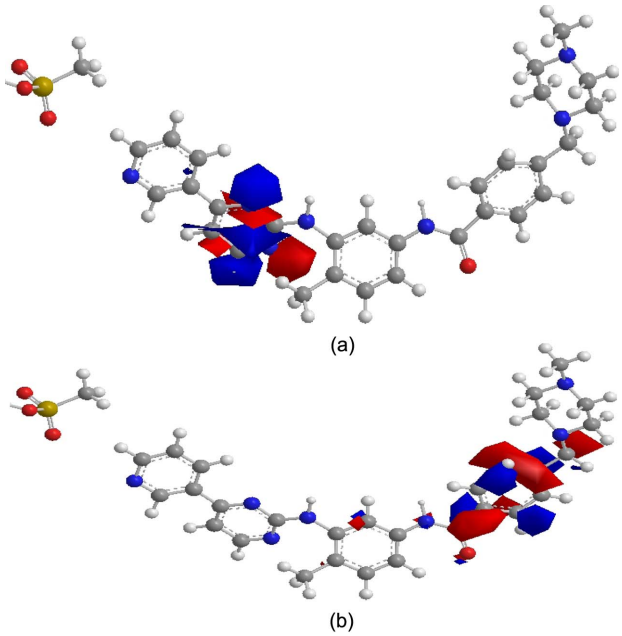

***Fig.* 9.** The Structure of molecular orbital plots of IMT: (a) HOMO orbital density (b) LUMO orbital density.

is that, IMT having approximate planar structure with larger molecular weight than usual inhibitors and this allows the molecule to have more functional groups which are in favor of corrosion inhibition.

FT-IR Analysis

The FT-IR analysis of IMT before and after reaction with iron was carried out between 400 and 4,000 cm^{-1} and the spectra are shown in *Figs.* 10a and10b, respectively. The peak around 3000-3050 cm^{-1} was assigned to C-H stretching, C=O and N-H stretching frequencies are shown at 1659 cm^{-1} and 3435 cm^{-1}, respectively. On com-

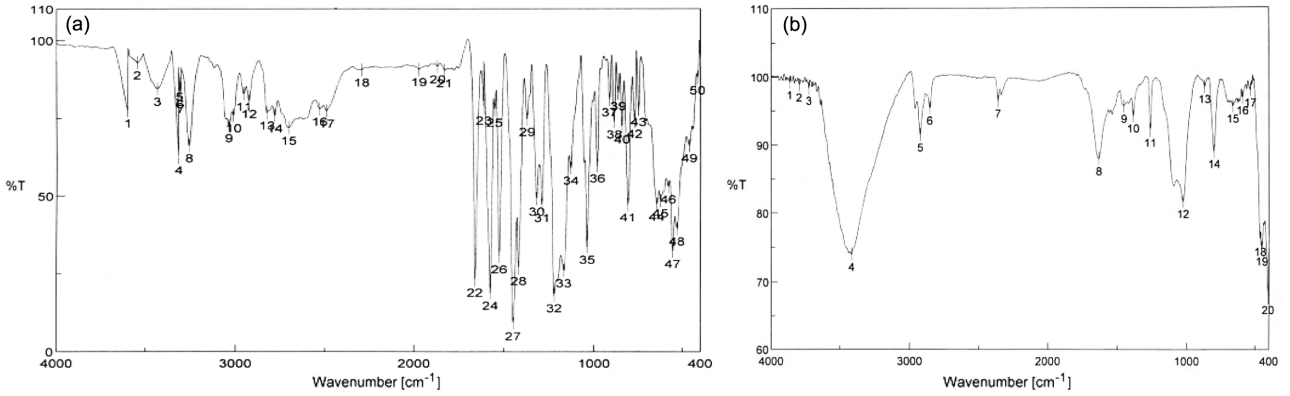

***Fig.* 10.** (a) as FT-IR spectrum of pure IMT before its reaction with iron at optimum conditions, (b) FT-IR spectrum of IMT after reaction with iron at optimum conditions.

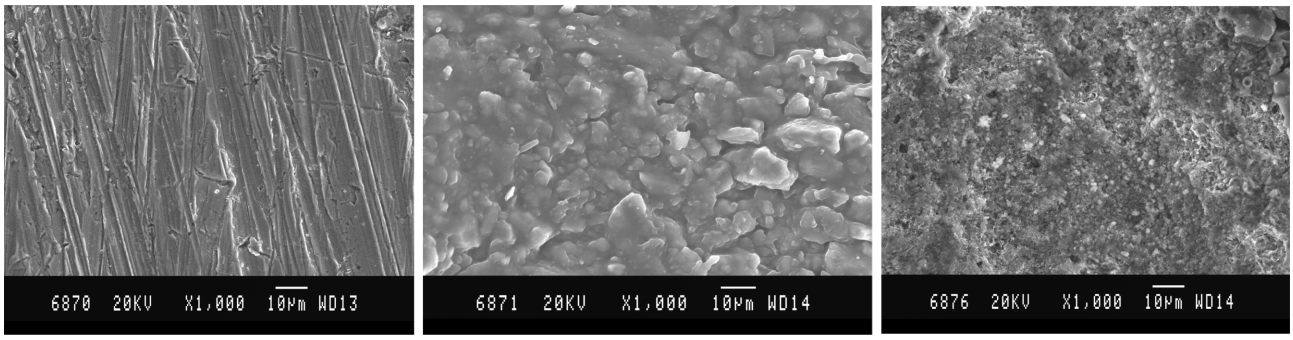

***Fig.* 11.** SEM images of Mild steel in 0.25 M H_2SO_4 after 6 h immersion at 70 ºC and at 1800 rpm (a) Before immersion (polished) (b) without inhibitor (c) with 5 mM IMT.

paring the spectrum of pure IMT with the spectrum of adsorbed IMT molecule over iron, it is observed that shifting of C=O stretching frequency from 1659 to 1629 cm^{-1} and disappearance of N-H stretching frequency indicating that there is interaction between the surface of mild steel and IMT.[46]

Morphological Investigation

The protective layer that formed on the metal surface was characterized by SEM analysis. Morphologies of mild steel in the absence and presence of optimum concentration of IMT at 70 ºC are shown in *Figs.* 11a - 11c. It can be seen from *Fig.* 11a that the mild steel samples before immersion seem smooth. Inspection of *Fig*. 11b reveals that the mild steel surface after immersion in uninhibited 0.25 M sulphuric acid for 6 h shows an aggressive attack of the corroding medium on the steel surface. The corrosion products appeared very uneven and lepidoteral-like morphology, and the surface layer is rather rough. In contrast, in the presence of IMT there is an adsorbed film on the metal surface (*Fig.* 11c).

CONCLUSIONS

1. Results obtained from the experimental data shows IMT as effective inhibitor for the corrosion of carbon steel in 0.25 M H_2SO_4.

2. The adsorption of IMT was found to obey the Langmuir adsorption isotherm.

3. The corrosion rate in the presence and in the absence of inhibitor decreased with increasing rotational speed up to 1800 rpm and then it began to increasing. The adsorbed film containing the investigated compound was identified by SEM analysis and FT-IR spectroscopy.

4. The lower values of activation energy in the presence of IMT than those in its absence, and the higher values of Gibbs free energy indicated that the adsorption of IMT on mild steel in 0.25 M sulphuric acid is chemisorption.

REFERENCES

1. Dubey, A. K.; Singh, G. *Port. Electrochim. Acta.* **2007**, *25*, 249.

2. Benali, O.; Larabi, L.; Mekelleche, S. M.; Harek, Y. *J. Mater. Sci*. **2006**, *41*, 7064.
3. Leila, H.; Balkheir, H.; Abdelouahad, A.; Sghir El, K.; Rachid, T. *Acta. Chim. Slov.* **2007**, *54*, 419.
4. Abd El Rehim, S. S.; Ibrahim Magdy, A. M.; Khalid, K. F. *Matter. Chem. Phys*. **2001**, *70*, 268.
5. Skyes, J. M. *Br. Corros. J*. **1990**, *25*, 175.
6. Shyamalay, M.; Arulanantham, A. *J. Mater. Sci. Technol*. **2009**, *25*, 5.
7. Benabdellah, M.; Rhomari, M.; Raada, A.; Dafali, A.; Senhaji, O.;Hammouti, B.; Aouniti, A.; Robin, J. J. *Chem. Eng. Comm*. **2007**, *194*, 1328.
8. Xianghong, L.; Deng, C.; Hui, F.; Guannan, M. *Corros. Sci*. **2008**, *50*, 3599.
9. Vishwanathan, S.; Haldar, N. *Corros. Sci*. **2008**, *50*, 2999.
10. Ali, S. A.; Al-Muallem, H. A.; Saeed, M. T.; Rahman, S. U. *Corros. Sci*. **2008**, *50*, 3070.
11. Siddiqi, W. A.; Chaubey, V. M. *Port. Electrochim. Acta*. **2008**, *26*, 221.
12. Peng, Z.; Cheng, Z.; Lei, H.; Lihong, N.; Fushi, Z. *Corros. Sci*. **2008**, *50*, 2166.
13. Prabhu, R. A.; Venkatesha, T. V.; Shanbhag, A.V. *J. Iran. Chem*. **2009**, *6*, 353.
14. Prabhu, R. A.; Venkatesha, T. V.; Shanbhag, A.V.; Praveen, B. M.; Kulkarni, G. M.; Kalkhambkar, R. G. *Matter. Chem. Phys*. **2008**, *108*, 283.
15. Haifeng, Y.; Yiping, S.; Jiahua, J.; Wei, S.; Xuan, Z.; Yanyan, Y.; Zongrang, Z. *Corros. Sci*. **2008**, *50*, 3160.
16. Yildirim, A.; Cetin, M. *Corros. Sci*. **2008**, *50*, 155.
17. Halperin, A.; Tirelli, M.; Lodge, T. P. *Adv. Polym. Sci*. **1992**, *100*, 31.
18. Abdallah, M. *Corros. Sci*. **2002**, *44*, 717.
19. Abdallah, M. *Corros. Sci.* **2004**, *46*, 1981.
20. El-Naggar, M. M. *Corros. Sci.* **2007**, *49*, 2226.
21. Lebrini, M.; Lagrenee, M.; Vezin, H. Traisnel, M.; Bentiss, F. *Corros. Sci*. **2007**, *49*, 2254.
22. Tang, L.; Mu, G.; Liu, G. *Corros. Sci*. **2003**, *45*, 2251.
23. Varsalovic, L.; Kliskic, M.; Radosevic, J.; Gudic, S. *J. Appl. Electrochem*. **2007**, *37*, 325.
24. Wei hua, L.; Qiao, H.; Sheng, T. Z.; Chang, L. P.; Bao, R. H. *J. Appl. Electrochem*. **2008**, *38*, 289.
25. Bouklah, M.; Hammouti, B.; Lagrenee, M.; Bentiss, F. *Corros. Sci*. **2006**, *48*, 2470.
26. Bayoumi, F. M.; Ghanem, W. A. *Matter. Lett*. **2005**, *59*, 3806.
27. Mohameed, A.; Amin. *J. Appl. Electrochem*. **2006**, *36*, 215.
28. Li, X.; Deng, S.; Fu, H.; Mu, G. *Corros. Sci*. **2009**, *51*, 620.
29. Aljourani, J.; Raeissi, K.; Golozar, M. A. *Corros. Sci*. **2009**, *51*, 1836.
30. Hoar, T. P.; Holliday, R. D. *J. Appl. Chem*. **1953**, *3*, 502.
31. Putilova, I. N.; Balzin, S. A.; Branik, U. P. *Metallic corrosion inhibitor*; Pergamon Press: 1960, p.3.
32. Nnabuk O. E.; Eno, E. E.; Udo J. I. *J. Appl.Electrochem.* **2010**, *40*, 445.
33. Szauer, T.; Brandt, A. *Electrochim. Acta*. **1981**, *26*, 1209.
34. Sankarapapavinasam, S.; Pushpanaden, F.; Ahmed, M. F. *Corros. Sci*. **1991**, *32*, 193.
35. Ivanov, E. S. *Inhibitors for Metal Corrosion in Acid Media*, Metallurgy, Moscow, **1986**.
36. Popova, A. *Corros. Sci*. **2007**, *49*, 2144.
37. Abdallah, M.; Heal, E. A.; Fouda, A. S. *Corros. Sci.* **2006**, *48*, 1639.
38. Abd El Rehim, S. S.; Refaey, S. A. M.; Taha, F.; Saleh, M. B.; Ahmed, R. A. *J. Appl. Electrochem*. **2001**, *31*, 429.
39. Yurt, A.; Balaban, A.; Kandemir, S. U.; Bereket, G.; Erk, B. *Mater. Chem. Phys*. **2004**, *85*, 420.
40. Tang, L.; Li, X.; Si, Y.; Mu, G.; Liu, G. *Mater. Chem. Phys.* **2006**, *95*, 26.
41. Gao, B. J.; Zhang, X.; Sheng, Y. L. *Mater. Chem. Phys*. **2008**, *108*, 375.
42. Yurt, A.; Bereket, G.; Kivrak, A.; Balban, A.; Erk, B. *J. Appl. Electrochem*. **2005**, *35*, 1025.
43. Gabriella, L. G.; Gabor, M.; Bela, L.; Gyorgy, J. *Corros. Sci*. **2003**, *45*, 1685.
44. Bouklah, M.; Hammouti, B.; Aouniti, A.; Benhadda, T. *Prog. Org. Coat*. **2004**, *49*, 225.
45. El Azhar, M.; Menari, B.; Traisnel, M.; Bentiss, F.; Lagrenee, M. *Corros. Sci*. **2003**, *43*, 2229.
46. Robinson, S. D.; Uttleys, M. F. *J. Chem. Soc.* **1973**, *12*, 1912.